

## 10. Nanoscale Materials and Fabrication Technology, Devices, and Systems

## ANALYSIS AND APPLICATIONS OF NANOSTRUCTURES CREATED BY STENCIL LITHOGRAPHY

O. Vázquez-Mena<sup>1</sup>, T. Sannomiya<sup>2</sup>, M. Tosun<sup>1</sup>, J. Voros<sup>2</sup>, G. Villanueva<sup>1</sup>, J. Brugger<sup>1</sup><sup>1</sup>The Microsystems Laboratory, Ecole Polytechnique Fédérale de Lausanne. Lausanne, SWITZERLAND<sup>2</sup>Laboratory of Biosensors and Bioelectronics, ETH Zurich. Zurich, SWITZERLAND

Stencil Lithography (SL) is a technique based on shadow mask deposition that does not require any resist processing, energy radiation or chemical solvents. This technique has been used to fabricate sub-micrometric structures, like nanodots [1] and nanowires [2]. It is suitable for patterning on substrates with high topographies, fragile structures and with materials damaged by radiation or solvents. SL also offers the potential for rapid nanopatterning of structures using the stencils several times [3]. However, SL still faces challenges for nanopatterning, like the blurring of the deposited structures due to the stencil-substrate gap [4]. Herein we show advances in the analysis, characterization and application of nanostructures deposited by SL.

In this contribution, we present a quantitative study of the blurring as a function of the gap. We show the patterning and electrical characteristics of Au nanowires deposited on polymer substrates by SL. Finally, we present the fabrication of Au nanodots and their use as biosensors based on localized surface plasmon resonance (LSPR)[5]. The stencils used for these experiments consist on silicon wafers with 100 nm thick low stress silicon nitride membranes containing nanoapertures.

The blurring in SL is due to the gap between stencil and substrate. To study this relation, we fabricated stencils with membranes having steps (with apertures) as shown in Figure 1.a. This allows us to have different and controlled gaps in a single evaporation with the same stencil. By depositing 60 nm of Al through nanoslits located at different steps of the membranes, nanowires were formed on the substrate. Figures 1.b-d show nanowires deposited through 180 nm wide apertures at different gaps showing a loss in resolution and thickness (Figure 1.e) as the gap increases. The blurring,

*Blurring = (WidthDepositedStructure) - (WidthStencilAperture),*

and thickness, are plotted as a function of the gap in Figure 1.f. It can be observed that for a gap of ~40µm, the blurring is about 80nm and the thickness reduced to ~50% of the nominal deposited thickness.

Using normal stencils (flat membranes), we have created nanowires (NW) and nanodot arrays. By depositing 45nm of Au through stencils containing nanoslits, we fabricated Au NWs on different polymer substrates: polyimide (PI), parylene and SU-8. The nanowires are deposited between predeposited Au electrodes to allow electrical measurements. We obtained wires up to 20µm long and

80nm wide as illustrated in Figure 2. The resistance as a function of width is shown in Figure 3. The resistivity obtained is ~10 µΩcm for parylene and SU-8, and ~7.5µΩcm for PI. These values are higher than bulk value (2.5µΩcm) due to size effects (grain and surface scattering).

We also used stencils with 50nm diameter holes to deposit arrays of 65nm diameter, 80nm thick Au nanodots (Figure 4.a and b). The total size of the array is ~20µm. We measured the extinction spectra due to LSPR (Figure 4.c) for arrays with different spacing between the nanodots, showing a resonance peak at 800nm. These structures were used to perform biosensing measurements based on the shift of the LSPR peak when biomolecules are added to metallic nanostructures. As expected, Figure 4.d shows a peak shift when biotin (PLL-PEG-biotin) binds to gold and then when streptavidin binds to biotin.

These results show that even at large gaps like 40 µm, it is possible to pattern nanostructures, but that reducing the gap increases significantly the definition of the structures. We have also shown the fabrication of nanowires with the expected ohmic behavior on plastic substrates. Similarly, the fabricated nanodots have been successfully applied for biosensing experiments using LSPR. This demonstrates the applications of nanostructures deposited by stencil lithography, opening new possibilities for nanopatterning.

Words: 597

## REFERENCES

- [1] M. M. Deshmukh, D. C. Ralph, M. Thomas, and J. Silcox, Applied Physics Letters, vol. 75, pp. 1631-1633, 1999.
- [2] O. Vazquez-Mena, G. Villanueva, V. Savu, K. Sidler, M. A. F. van den Boogaart, and J. Brugger, Nano Letters, vol. 8, pp. 3675-3682, 2008.
- [3] O. Vázquez-Mena, G. Villanueva, M. A. F. van den Boogaart, V. Savu, and J. Brugger, Microelectronic Engineering, vol. 85, pp. 1237-1240, 2008.
- [4] M. Lishchynska, V. Bourenkov, M. A. F. van den Boogaart, L. Doeswijk, J. Brugger, and J. C. Greer, Microelectronic Engineering, vol. 84, pp. 42-53, 2007.
- [5] J. N. Anker, W. P. Hall, O. Lyandres, N. C. Shah, J. Zhao, and R. P. Van Duyne, Nat Mater, vol. 7, pp. 442-453, 2008.

Contacts: [juergen.brugger@epfl.ch](mailto:juergen.brugger@epfl.ch), [oscar.vazquez@epfl.ch](mailto:oscar.vazquez@epfl.ch)

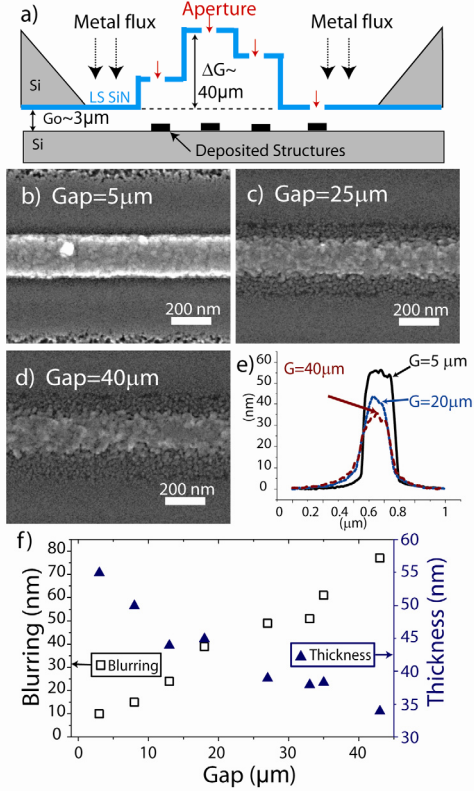


Figure 1. (a) Schematics of stencil membrane with steps, producing different gaps with the same stencil.  $G_0$  corresponds to an offset gap between stencil and substrate (measured value:  $\sim 3 \mu\text{m}$ ). (b-d) Aluminum structures deposited through 180 nm wide apertures located at different steps of the stencil. A loss in resolution is observed as the gap increases. (e) AFM profile of the previous structures. (f) Blurring and thickness as a function of gap.

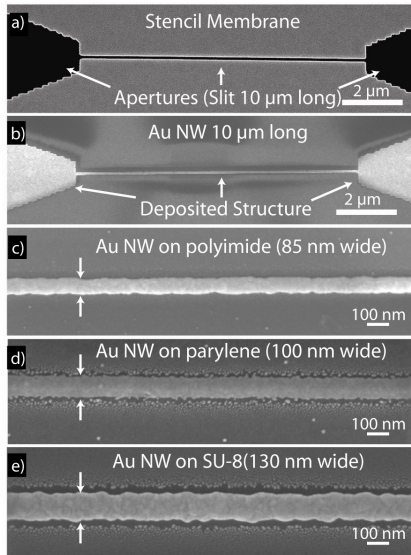


Figure 2. (a) SEM image of a stencil aperture in a LS SiN membrane. (b) Au nanowire deposited on PI through the aperture in (a). (c-e) 45 nm thick NWs deposited through a stencil on PI, parylene and SU8 substrates.

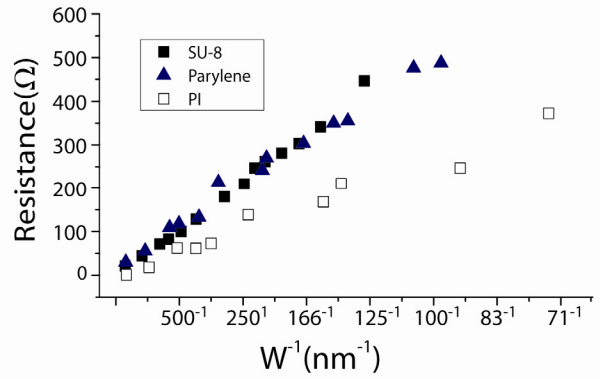


Figure 3. Resistance as function of the inverse of the width for Au nanowires deposited on PI, parylene and SU-8. The extracted resistivities are:

$$-\rho_{\text{Au on parylene}} \sim \rho_{\text{Au on SU-8}} \sim 10 \mu\Omega \text{ cm}$$

$$-\rho_{\text{Au on PI}} \sim 7.5 \mu\Omega \text{ cm}$$

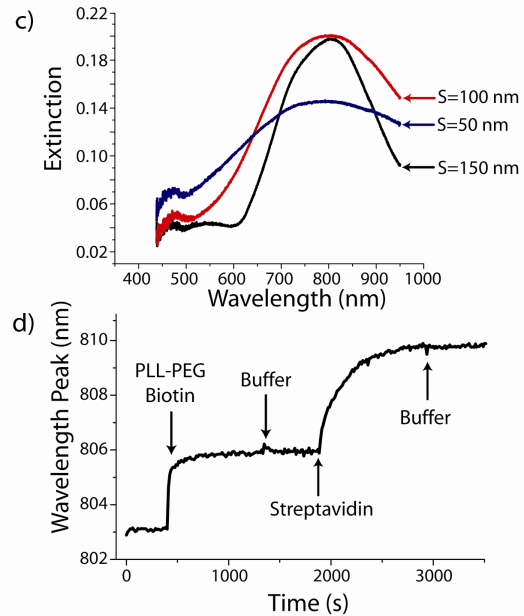
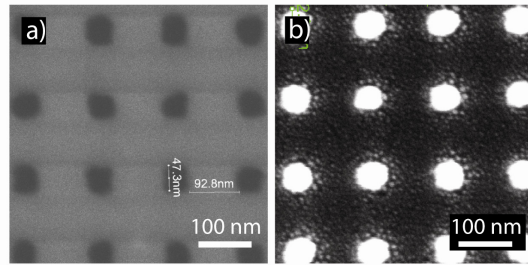


Figure 4. (a) Stencil containing 50 nm wide holes array. (b) 65 nm in diameter, 80 nm thick Au dots deposited through the stencil in (a). (c) LSPR extinction spectra for three arrays with Au dots 65 nm in diameter and spacing between dots of: 50, 100 and 150 nm. For smaller spacing between dots, the resonance peak is broader. (d) Response of the Au dot array (dot size: 65 nm, spacing: 150 nm) when adding biotin and streptavidin. Buffer: pH 7.4, PLL-PEG-Biotin: 100  $\mu\text{g/ml}$ , Streptavidin: 20  $\mu\text{g/ml}$